

Supplementary information

Biomechanical insights into the dentition of megatooth sharks (Lamniformes: Otodontidae)

Antonio Ballell¹, and Humberto G. Ferrón^{1,*}

¹Shool of Earth Sciences, University of Bristol, Bristol BS8 1RJ, UK.

*humberto.ferron@bristol.ac.uk

This file includes:

Supplementary Figure 1. Von Mises stress distribution plots in the anterior (*Ant.*), lateral (*Lat.*), and posterior (*Post.*) teeth of the five analysed otodontid species, simulating puncture scenario with life-size absolute force estimates.

Supplementary Figure 2. Mesh-weighted average von Mises stress (MWAM) values calculated for anterior, lateral, and posterior teeth of the five analysed otodontid species, simulating puncture and draw scenarios with scaled force magnitude. This parameter was determined considering finite elements in the crown tooth.

Supplementary Figure 3. Tooth sets of the different otodontid species considered in our study.

Supplementary Figure 4. Convergence test results showing the variation of the mesh-weighted average von Mises (MWAM) stress respect to element size.

Supplementary Table 1. Details of planar models, tooth height, and body dimensions considered in the present study.

Supplementary Table 2. Summary of mesh parameters.

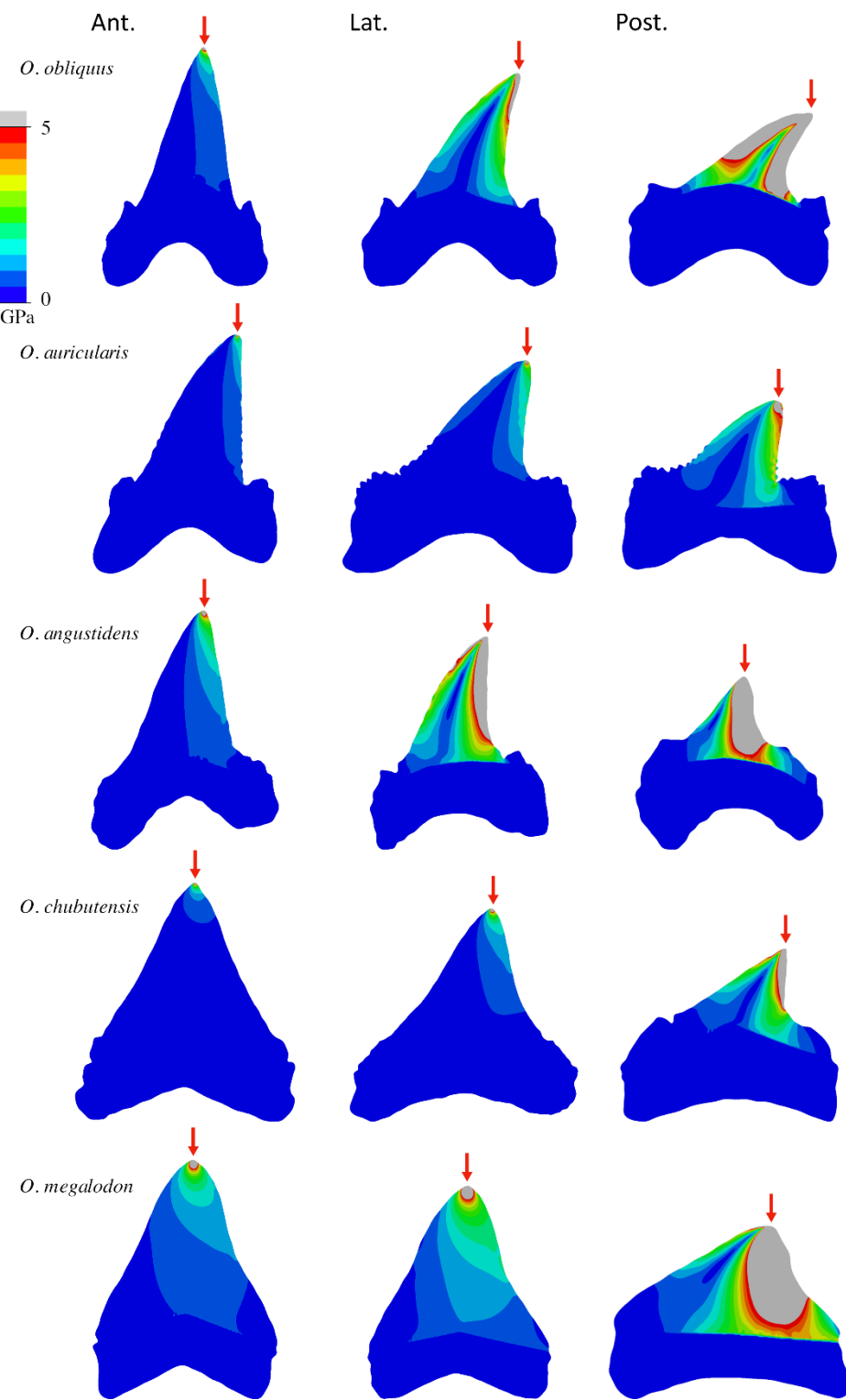
Supplementary Table 3. Finite element model characteristics and loading scenarios. *F* force, *SA* surface area.

Supplementary References

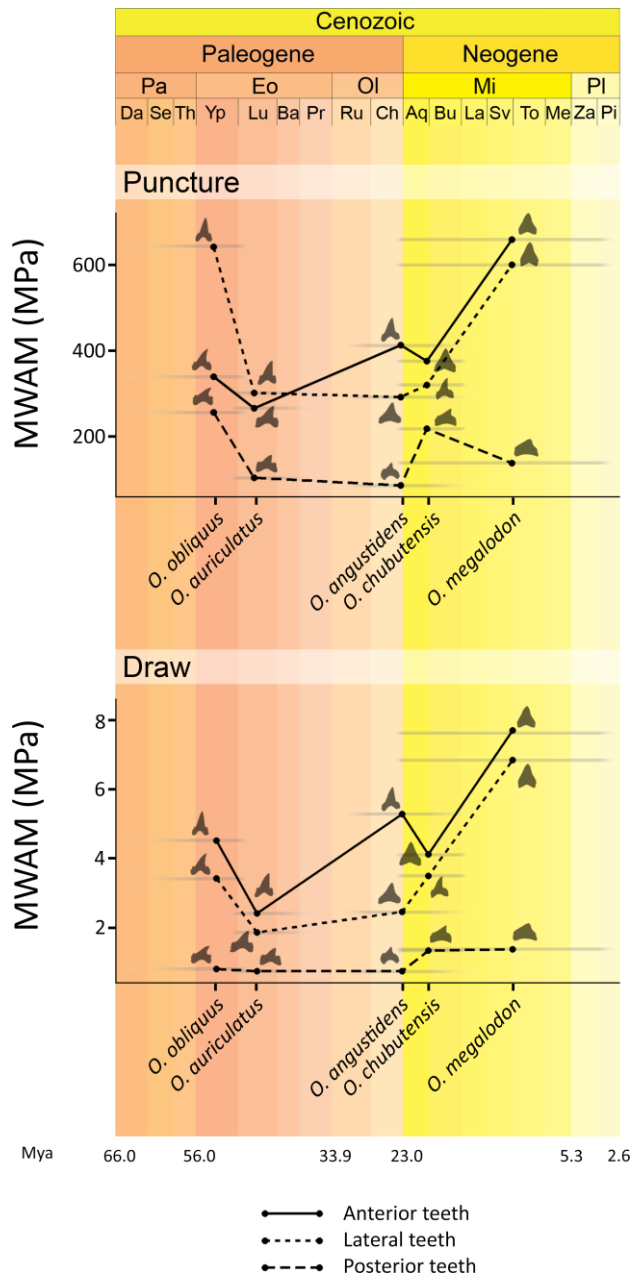
Other supplementary materials include (available at the Open Science platform Figshare):

Supplementary Data 1. STP files of planar models.

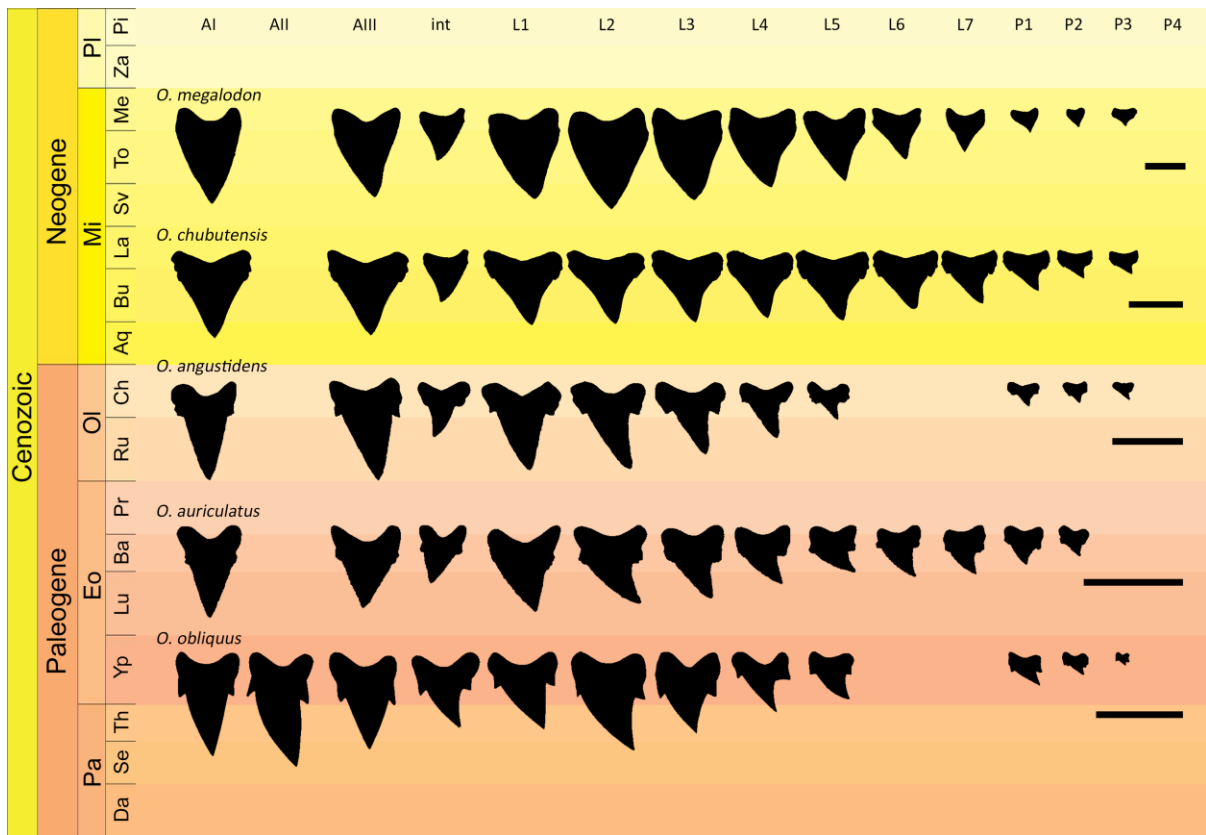
Supplementary Data 2. R code and associated files.



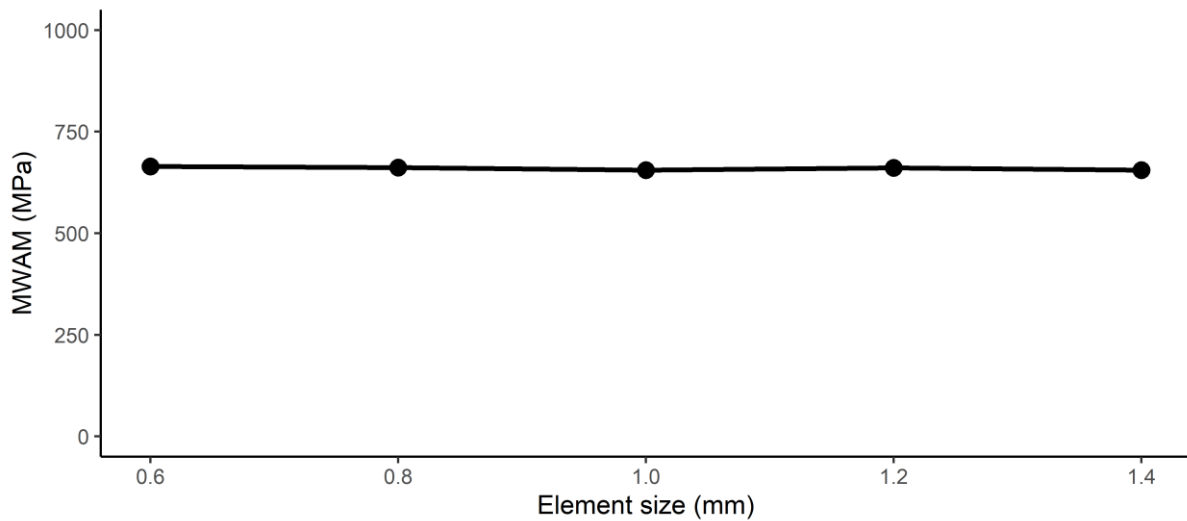
Supplementary Figure 1. Von Mises stress distribution plots in the anterior (*Ant.*), lateral (*Lat.*), and posterior (*Post.*) teeth of the five analysed otodontid species, simulating puncture scenario with life-size absolute force estimates. Mesial is left, distal is right. Arrows indicate loading points. Grey areas represent von Mises stress values higher than 5 GPa.



Supplementary Figure 2. Mesh-weighted average von Mises stress (MWAM) values calculated for anterior, lateral, and posterior teeth of the five analysed otodontid species, simulating puncture and draw scenarios with scaled force magnitude. This parameter was determined considering finite elements in the crown tooth. Data are shown in a temporal context (in million years ago, *Mya*) where stratigraphic range of each taxa is represented by grey bars (stratigraphic ranges based on Cappetta¹ and Diedrich²). Epoch: Pa, Paleocene; Eo, Eocene; Ol, Oligocene; Mi, Miocene; Pl, Pliocene; Age: Da, Danian; Se, Selandian; Th, Thanetian; Yp, Ypresian; Lu, Lutetian; Ba, Bartonian; Pr, Priabonian; Ru, Rupelian; Ch, Chattian; Aq, Aquitanian; Bu, Burdigalian; La, Langhian; Sv, Serravalian; To, Tortonian; Me, Messinian; Za, Zanclean; Pi, Piacenzian.



Supplementary Figure 3. Tooth sets of the different otodontid species considered in our study illustrating the morphology of anterior (A), lateral (L), intermediate (int) and posterior (P) teeth. Otodontid dentitions show a clear monognathic heterodonty (i.e., the morphology of their teeth varies depending on their position along the jaw). Thus, crowns of anterior teeth (situated close to the symphysis, left) are gracile and elongated while those of posterior teeth (situated close the commissures, right) are shorter and more robust. Lateral teeth show intermediate morphologies. Tooth set drawings modified from Perez et al.³ and Applegate & Espinosa-Arrubarrena⁴. Epoch: Pa, Paleocene; Eo, Eocene; Ol, Oligocene; Mi, Miocene; Pl, Pliocene; Age: Da, Danian; Se, Selandian; Th, Thanetian; Yp, Ypresian; Lu, Lutetian; Ba, Bartonian; Pr, Priabonian; Ru, Rupelian; Ch, Chattian; Aq, Aquitanian; Bu, Burdigalian; La, Langhian; Sv, Serravalian; To, Tortonian; Me, Messinian; Za, Zanclean; Pi, Piacenzian. Scale bars equal 5 cm.



Supplementary Figure 4. Convergence test results showing the variation of the mesh-weighted average von Mises (MWAM) stress respect to element size. Percentage error below 1 in all cases (see Supplementary Data S2).

	<i>Tooth</i>	<i>Planar model reference</i>	<i>Tooth height (cm)</i>	<i>Tooth height source</i>	<i>Body length (m)</i>	<i>Body length reference</i>	<i>Body mass (kg)</i>
<i>O. obliquus</i>	A	Gordon Hubbell collection (ds1001 UA1)	6.7	Gordon Hubbell collection natural tooth set	600	Biton-Porsmoguer ⁵	2162.96
	L	Gordon Hubbell collection (ds1001 UL2)	5.4	Gordon Hubbell collection natural tooth set	600	Biton-Porsmoguer ⁵	2162.96
	P	Gordon Hubbell collection (ds1001 UL10)	1.7	Gordon Hubbell collection natural tooth set	600	Biton-Porsmoguer ⁵	2162.96
<i>O. auriculatus</i>	A	Diedrich ² : fig. 3: 1	4.7	Applegate and Espinosa-Arrubarrena ⁴	400	Applegate and Espinosa-Arrubarrena ⁴	597.22
	L	Cappetta ¹ : fig. 209 H-J	3.7	Applegate and Espinosa-Arrubarrena ⁴	400	Applegate and Espinosa-Arrubarrena ⁴	597.22
	P	Cappetta ¹ : fig. 209 M-N	1.6	Applegate and Espinosa-Arrubarrena ⁴	400	Applegate and Espinosa-Arrubarrena ⁴	597.22
<i>O. angustidens</i>	A	Gottfried and Fordyce ⁶ : fig 3A	10.4	Gottfried and Fordyce ⁶	900	Gottfried and Fordyce ⁶	7833.60
	L	Gottfried and Fordyce ⁶ : fig 3F	4.3	Gottfried and Fordyce ⁶	900	Gottfried and Fordyce ⁶	7833.60
	P	Gottfried and Fordyce ⁶ : fig 3I	1.9	Gottfried and Fordyce ⁶	900	Gottfried and Fordyce ⁶	7833.60
<i>O. chubutensis</i>	A	Perez et al. ³ : fig. 5	8.8	Perez et al. ³	600	Perez et al. ³	2162.96
	L	Perez et al. ³ : fig. 5	7.3	Perez et al. ³	600	Perez et al. ³	2162.96
	P	Perez et al. ³ : fig. 5	2.9	Perez et al. ³	600	Perez et al. ³	2162.96
<i>O. megalodon</i>	A	Gordon Hubbell collection (ds1022 UA1)	16.8	Applegate and Espinosa-Arrubarrena ⁴	1500	Shimada ⁷	39637.80
	L	Gordon Hubbell collection (ds1022 UL3)	15	Gordon Hubbell collection natural tooth set	1500	Shimada ⁷	39637.80
	P	Gordon Hubbell collection (ds1022 UL8)	3.2	Gordon Hubbell collection natural tooth set	1500	Shimada ⁷	39637.80

Supplementary Table 1. Details of planar models, tooth height, and body dimensions considered in the present study. In *O. chubutensis* and *O. megalodon*, lateral and posterior tooth heights were extrapolated according to the proportions in the tooth sets from Perez et al.³ and Gordon Hubbell collection. For this, the largest tooth record reported in the literature was considered as the anterior tooth height in these species.

Taxon	Tooth	Element size (mm)	Number of elements	Number of nodes
<i>O. obliquus</i>	Anterior	0.30	33046	16869
<i>O. obliquus</i>	Lateral	0.30	29323	14984
<i>O. obliquus</i>	Posterior	0.10	40348	20527
<i>O. auriculatus</i>	Anterior	0.20	42787	21770
<i>O. auriculatus</i>	Lateral	0.20	42922	21834
<i>O. auriculatus</i>	Posterior	0.10	39775	20238
<i>O. angustidens</i>	Anterior	0.50	31453	16041
<i>O. angustidens</i>	Lateral	0.20	37739	19218
<i>O. angustidens</i>	Posterior	0.10	41985	21327
<i>O. chubutensis</i>	Anterior	0.40	31655	16111
<i>O. chubutensis</i>	Lateral	0.40	36730	18676
<i>O. chubutensis</i>	Posterior	0.20	32436	16507
<i>O. megalodon</i>	Anterior	0.90	33342	16950
<i>O. megalodon</i>	Lateral	0.80	36798	18689
<i>O. megalodon</i>	Posterior	0.25	30110	15312

Supplementary Table 2. Summary of mesh parameters.

Taxon	Tooth	SA (m^2)	Puncture		Draw		
			F (N) absolute	F (N) scaled	F (N)	Nodes in load	F (N) per node
<i>O. obliquus</i>	Anterior	1.43E-03	6988	5369	55	165	0.332
<i>O. obliquus</i>	Lateral	1.27E-03	10324	4759	49	126	0.385
<i>O. obliquus</i>	Posterior	1.95E-04	13661	732	7	127	0.059
<i>O. auriculatus</i>	Anterior	8.27E-04	2950	3103	32	175	0.181
<i>O. auriculatus</i>	Lateral	7.83E-04	4359	2937	30	133	0.225
<i>O. auriculatus</i>	Posterior	1.80E-04	5767	674	7	109	0.063
<i>O. angustidens</i>	Anterior	3.79E-03	16552	14219	145	161	0.900
<i>O. angustidens</i>	Lateral	7.27E-04	24456	2726	28	149	0.187
<i>O. angustidens</i>	Posterior	2.02E-04	32360	757	8	158	0.049
<i>O. chubutensis</i>	Anterior	3.76E-03	6988	14099	144	146	0.984
<i>O. chubutensis</i>	Lateral	2.83E-03	10324	10625	108	149	0.727
<i>O. chubutensis</i>	Posterior	6.23E-04	13661	2339	24	110	0.217
<i>O. megalodon</i>	Anterior	1.31E-02	49051	49051	500	162	3.086
<i>O. megalodon</i>	Lateral	1.15E-02	72481	43207	440	164	2.686
<i>O. megalodon</i>	Posterior	9.11E-04	95911	3418	35	98	0.356

Supplementary Table 3. Finite element model characteristics and loading scenarios. *F* force,

SA surface area.

Supplementary references

1. Cappetta, H. Chondrichthyes—Mesozoic and Cenozoic Elasmobranchii: Teeth (Verlag F, Pfeil, 2012).
2. Diedrich, C. White and megatooth shark evolution and predation origin onto seals, sirenians and whales. *Nat. Sci.* **5**, 1203-1218 (2013).
3. Perez, V. J., Godfrey, S. J., Kent, B. W., Weems, R. E. & Nance, J. R. The transition between *Carcharocles chubutensis* and *Carcharocles megalodon* (Otodontidae, Chondrichthyes): lateral cusplet loss through time. *J. Vertebr. Paleontol.* **38**, e1546732 (2018).
4. Applegate, S. P. & Espinosa-Arrubarrena, L. The fossil history of *Carcharodon* and its possible ancestor, *Cretolamnia*: A study in tooth identification. In *Great White Sharks: The Biology of Carcharodon carcharias, Ch 4* (eds Klimley, A. P. & Ainley, D. G.) (Academic Press, San Diego, 1996).
5. Biton-Porsmoguer, S. Posible área de reproducción de *Otodus obliquus* (Lamniformes: Lamnidae) del Paleoceno en la cuenca de Ganntour (Marruecos). *UMC hal-01660273* (2017).
6. Gottfried, M. D. & Fordyce, R. E. An associated specimen of *Carcharodon angustidens* (Chondrichthyes, Lamnidae) from the Late Oligocene of New Zealand, with comments on *Carcharodon* interrelationships. *J. Vertebr. Paleontol.* **21**, 730-739 (2001).
7. Shimada, K. The size of the megatooth shark, *Otodus megalodon* (Lamniformes: Otodontidae), revisited. *Hist. Biol.* 1-8 (2019).